Phycologia

Phycologia

ISSN: 0031-8884 (Print) 2330-2968 (Online) Journal homepage: https://www.tandfonline.com/loi/uphy20

Ultrastructure of the marine benthic dinoflagellate *Plagiodinium belizeanum* (Dinophyceae) from the southeast Pacific island of Okinawa, Japan

Kevin C. Wakeman, Mona Hoppenrath, Aika Yamaguchi, Greg S. Gavelis, Brian S. Leander & Hisayoshi Nozaki

To cite this article: Kevin C. Wakeman, Mona Hoppenrath, Aika Yamaguchi, Greg S. Gavelis, Brian S. Leander & Hisayoshi Nozaki (2018) Ultrastructure of the marine benthic dinoflagellate *Plagiodinium belizeanum* (Dinophyceae) from the southeast Pacific island of Okinawa, Japan, Phycologia, 57:2, 209-222, DOI: 10.2216/17-43.1

To link to this article: https://doi.org/10.2216/17-43.1

Published online: 08 Mar 2019.

Phycologia Volume 57 (2), 209–222 Published 11 January 2018

Ultrastructure of the marine benthic dinoflagellate *Plagiodinium belizeanum* (Dinophyceae) from the southeast Pacific island of Okinawa, Japan

Kevin C. Wakeman[1,2]*†, Mona Hoppenrath[3]†, Aika Yamaguchi[4], Greg S. Gavelis[5], Brian S. Leander[5] and Hisayoshi Nozaki[6]

[1]*Active Learning of English for Science Students (ALESS) Program, Center for Global Communication Strategies, Komaba Campus, University of Tokyo, Tokyo, Japan*
[2]*Institute for International Collaboration, Hokkaido University, Sapporo, Hokkaido, Japan*
[3]*Senckenberg am Meer, German Center for Marine Biodiversity Research, Wilhelmshaven, Germany*
[4]*Research Center for Inland Seas, Kobe University, Kobe, Japan*
[5]*Department of Zoology, University of British Columbia, Vancouver, British Columbia, Canada*
[6]*Department of Biological Sciences, Graduate School of Science, University of Tokyo, Tokyo, Japan*

Abstract: We isolated *Plagiodinium belizeanum* into clonal culture from the Pacific island of Okinawa (Japan) and characterized it using a combination of light microscopy, scanning electron microscopy, transmission electron microscopy and 18S/28S ribosomal (r) gene sequences. Although molecular phylogenetic analyses of 18S rDNA and 28S rDNA sequences were unable to resolve the phylogenetic position of *P. belizeanum* within dinoflagellates, the ultrastructural data provided some new traits for the species. For instance, double-membrane-bound vesicles, distinct from the mitochondria, were interpreted as autolysosomes containing electron-dense virus particles. The thecal plate pattern was Po 1′ 0a 5′′ 5(6)C 4S 5′′′ 0p 1′′′′, which is slightly different from the original description in having an additional epithecal plate and four sulcal plates. The laterally flattened cells were 22–34 μm long, 11–13 μm deep, and 15–18 μm wide and contained a peridinin-type plastid with lobes radiating from a central pyrenoid that lacked starch sheaths and was traversed by stacks of thylakoids. This isolate represents the first record of the species in Japan, and the new ultrastructural and DNA sequence data were used to emend the species description.

Key Words: Classification, Epifluorescence, *Madanidinium, Pileidinium, Planodinium, Pseudadenoides, Sabulodinium,* Scanning electron microscopy, Taxonomy, *Thecadinium kofoidii,* Transmission electron microscopy, Ultrastructure

INTRODUCTION

Approximately 190 of the 2500 described species of dinoflagellates live in marine benthic habitats (Taylor *et al.* 2008; Hoppenrath *et al.* 2014; Hoppenrath 2017). The diversity, biogeography and ecology of these species remain poorly understood. Of the 45 recognized genera, several thecate taxa have unusual and difficult-to-interpret thecal plate patterns (Hoppenrath *et al.* 2014): *Adenoides* Balech emend. F.Gómez, R.Onuma, Artigas & Horiguchi (Gómez *et al.* 2015), *Ailadinium* Saburova & Chomérat (Saburova & Chomérat 2014), *Amphidiniella* Horiguchi (Horiguchi 1995), *Cabra* Murray & Patterson emend. Chomérat, Couté & Nézan (Murray & Patterson 2004; Chomérat *et al.* 2010), *Pileidinium* Tamura & Horiguchi (Tamura & Horiguchi 2005) and *Rhinodinium* Murray, Hoppenrath, Yoshimatsu, Toriumi & Larsen (Murray *et al.* 2006). These ambiguous morphological traits combined with poorly resolved molecular phylogenetic relationships of dinoflagellates as a whole make the classification of these species tenuous at best (Hoppenrath *et al.* 2014). The thecal plate patterns in laterally flattened species with a small epitheca are especially difficult to interpret. Lineages such as *Planodinium* Saunders & Dodge (Saunders & Dodge 1984; Hoppenrath *et al.* 2014), *Sabulodinium* Saunders & Dodge emend. Hoppenrath, Horiguchi, Miyoshi, Selina, Taylor & Leander (Saunders & Dodge 1984; Hoppenrath *et al.* 2007) and *Sinophysis* Nie & Wang emend. Chomérat (Chomérat 2016) often have incomplete reconstructions of their epitheca and sulcal regions, for this reason.

The tabulation pattern of the laterally flattened cells of *Plagiodinium* Faust & Balech, with the type *P. belizeanum* Faust & Balech, was previously characterized using light microscopy (LM) and scanning electron microscopy (SEM) (Faust & Balech 1993): Po 5′ 0a 0′′ 5C 5S 5′′′ 0p 1′′′′. However, details associated with the small epithecal and sulcal plates were not discernible on the scanning electron micrographs (Faust & Balech 1993). Because of these ambiguities, Hoppenrath *et al.* (2014) suggested that the species is in need of reinvestigation. Only a few observations of *P. belizeanum* have been published since its original description from floating detritus, coral rubble and mangrove sediments in Twin Cays, Belize (Faust & Balech 1993). Reports from the Yucatan Peninsula (Okolodkov *et al.* 2014), the Mexican Caribbean (Almazán-Becerril *et al.* 2015) and Japan (Yamada *et al.* 2015) included only light micrographs demonstrating the general morphology that did not add further morphological information to the species description. The aim of the current study was to cultivate a new isolate of *P. belizeanum* and combine molecular phylogenetic data, ultrastructural data and biogeographical data with the original description of the species.

* Corresponding author (wakeman.kevin@gmail.com).
† These authors contributed equally to the manuscript.
DOI: 10.2216/17-43.1

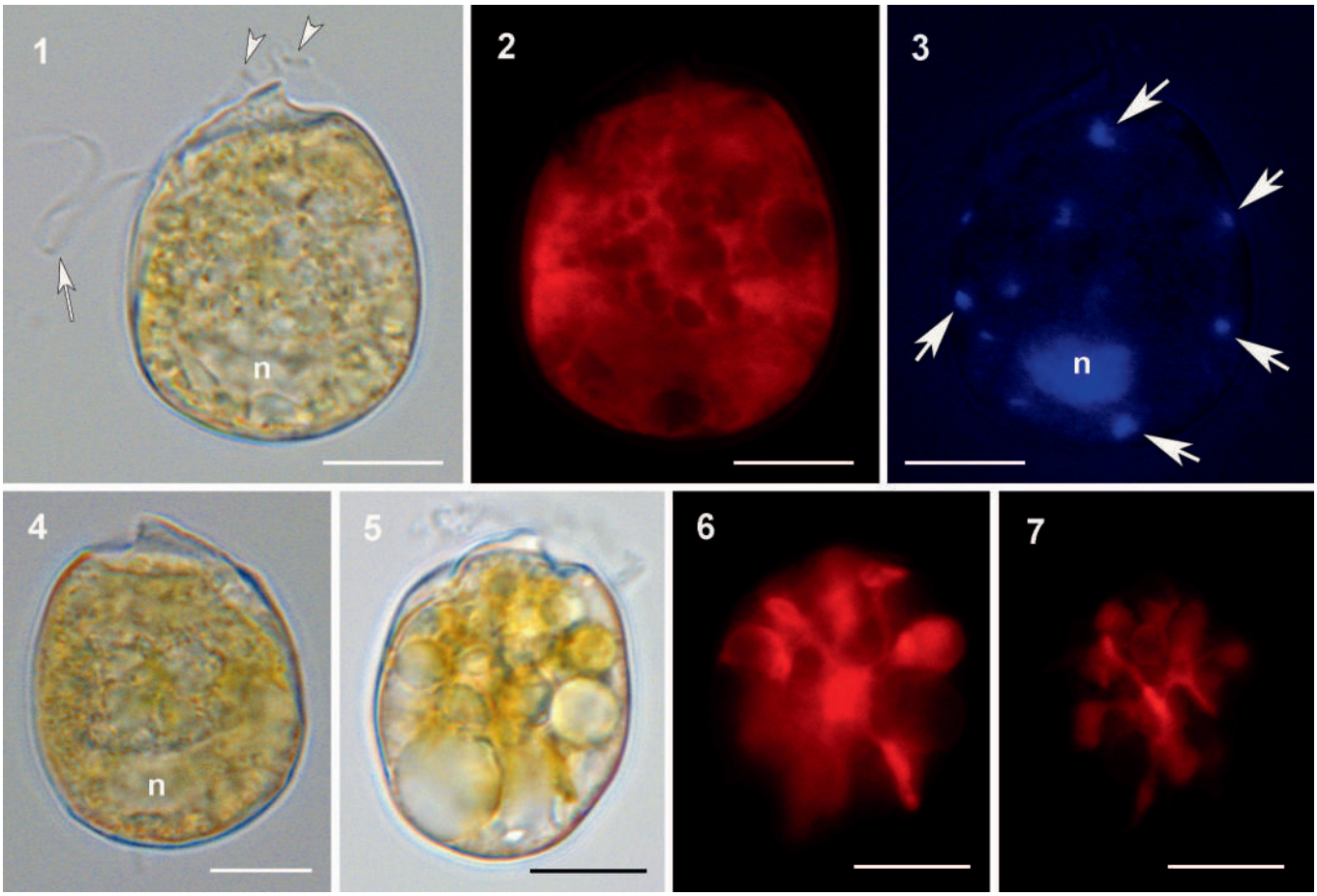

Figs 1–7. Light micrographs of *Plagiodinium belizeanum*. Scale bars = 10 μm.
Figs 1–3. Same cell.
Fig. 1. Living cell seen from the left lateral side with visible longitudinal (arrow) and transverse flagellum (arrowheads). Note the posteriorly located nucleus (n).
Figs 2, 3. Epifluorescence images.
Fig. 2. Autofluorescence of the plastids.
Fig. 3. DAPI staining showing the nucleus (n) and putative autolysosomes containing virus particles (arrows).
Fig. 4. Living cell seen from the right lateral side; note the nucleus (n).
Figs 5–7. Same cell.
Fig. 5. Living cell containing starch granules of different sizes.
Figs 6, 7. Different focal planes showing autofluorescence of the plastids radiating from the cell centre.

MATERIAL AND METHODS

Sand was collected at a depth of 2 m while snorkeling at Odo, Itoman, Okinawa, Japan (26°04.29′N, 127°40.37′E) on 15 April 2015. The top layer of the sand–seawater samples was pipetted into an observation well where individual cells of *Plagiodinium belizeanum* were isolated and washed in filtered seawater using hand-drawn glass pipettes. A clonal culture was established on 16 April 2015 by placing single cells into a 24-well tissue culture plate containing 0.125 g l^{-1} (powder) Daigo's IMK culture media in autoclaved, filtered seawater. *Plagiodinium belizeanum* was maintained at 25°C in a 12:12 light:dark cycle (100 photons m^{-2} s^{-1}). The culture was deposited at the Hokkaido University Culture Collection in the Faculty of Science under the designation KW001.

LM and electron microscopy were done with a culture that was about 2 mo old. Differential interference contrast images of motile cells of *Plagiodinium belizeanum* were taken using an Olympus BX-53 microscope (Olympus, Tokyo, Japan) attached to an Olympus DP71 digital camera. For fluorescent imaging, some cells were fixed in 2.5% glutaraldehyde (Sigma-Aldrich, St. Louis, Missouri USA) in culture media. A drop of 1% 4′,6-diamidino-2′-phenylindole (DAPI) (Sigma-Aldrich) stained DNA in the cell. For SEM 1.5 ml of culture was transferred to a 1.5-ml Eppendorf tube and fixed at room temperature with 15 μl of acidic Lugol's solution. Cells remained in the Lugol's media mixture for 2 wk before being mounted on a round coverslip using poly-L-lysine (Sigma-Aldrich), washed with distilled water and dehydrated through a graded series of ethanol (30, 50, 75, 80, 90, 95 and 100%; 5 min at each step). Samples were critical-point dried with CO_2, sputter coated with 5 nm of gold and viewed using a Hitachi 4700 electron microscope (Hitachi, Tokyo, Japan).

Additionally, Lugol-fixed culture material was placed on a 5-μm Millipore filter, rinsed in distilled water and dehydrated in a series of increasing ethanol concentrations (30, 50, 70, 85,

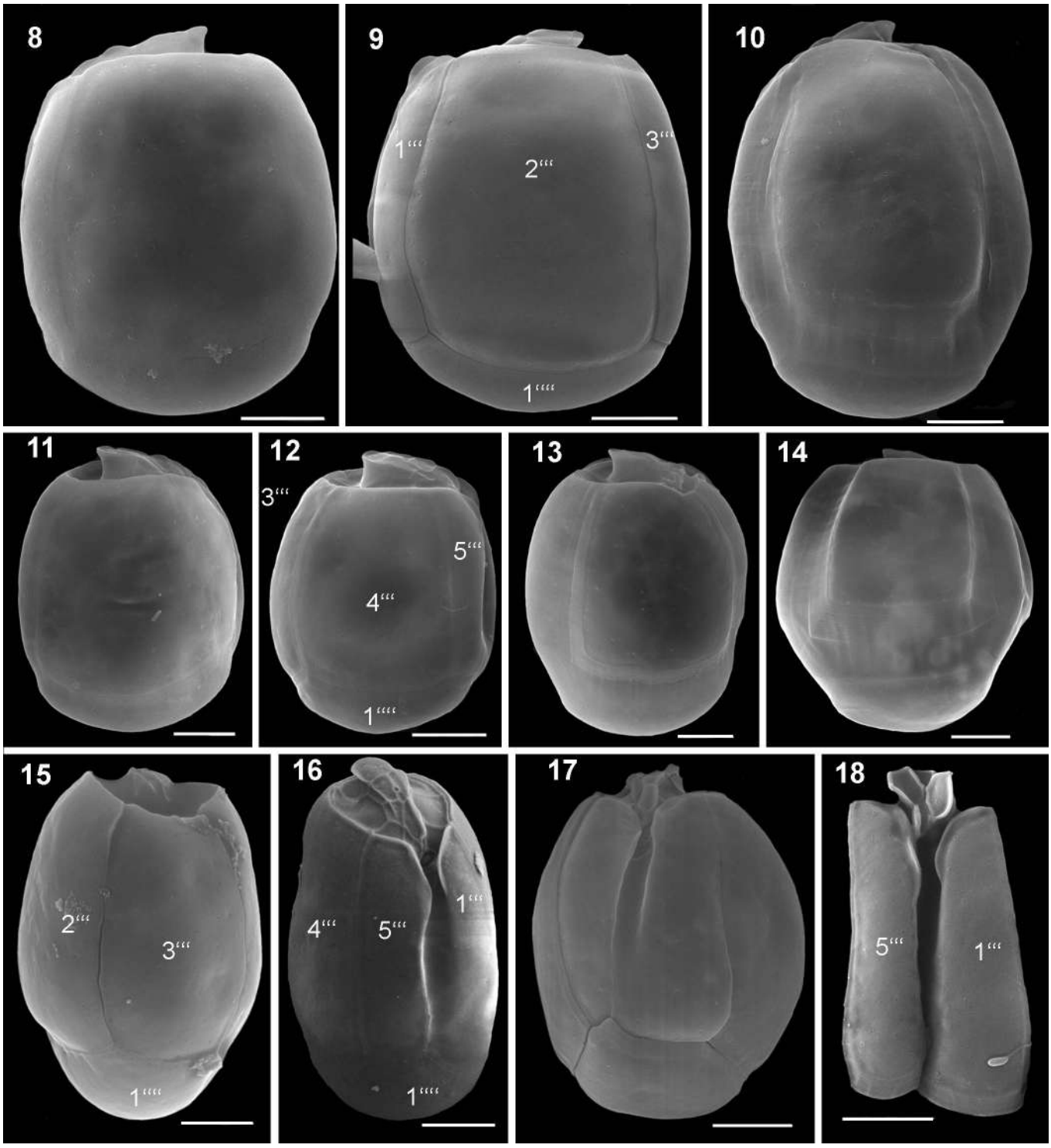

Figs 8–18. Scanning electron micrographs of *Plagiodinium belizeanum*. Scale bars = 5 μm.
Figs 8–10. Left lateral views of cells of different shape and intercalary band development.
Figs 11–14. Right lateral views of cells of different shape, size and intercalary band development.
Fig. 15. Dorsal view.
Figs 16, 17. Ventral views of cells of different shape and intercalary band development.
Fig. 18. Isolated plates from the ventral theca.

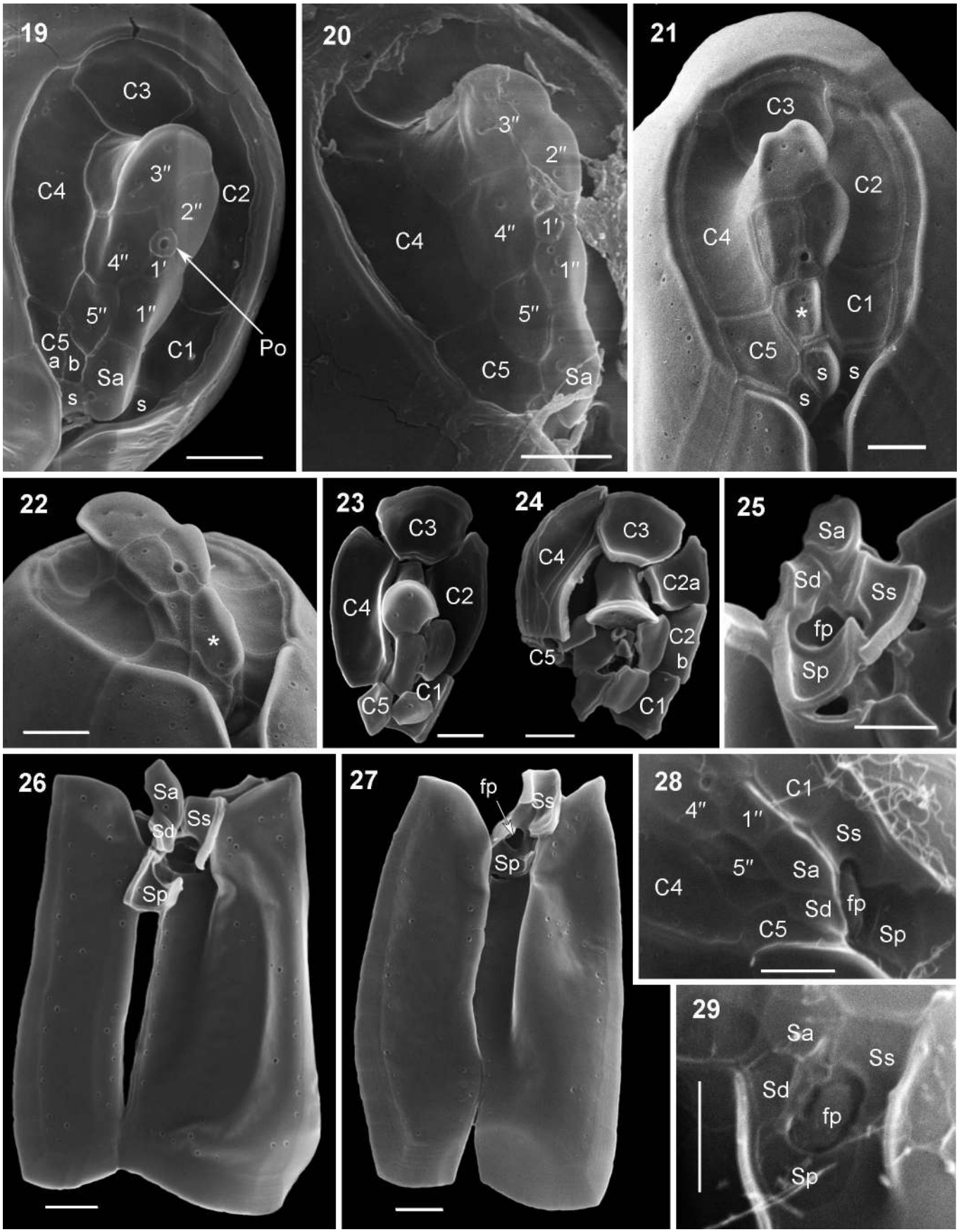

Figs 19–29. Scanning electron micrographs of *Plagiodinium belizeanum*. Scale bars = 2 μm.

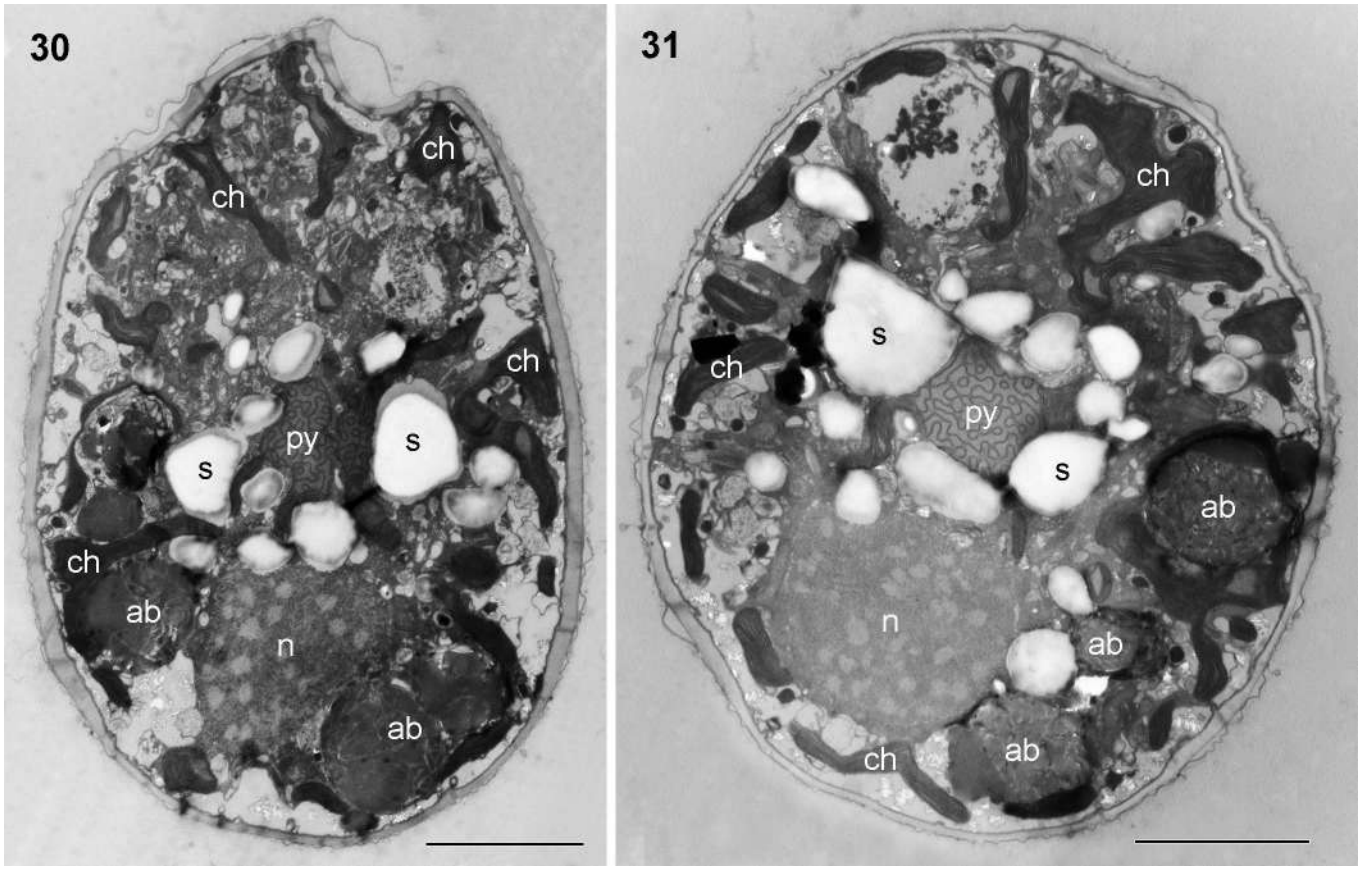

Figs 30, 31. Transmission electron micrographs of *Plagiodinium belizeanum*. ab = accumulation body; ch = plastid; n = nucleus; py = pyrenoid; s = starch. Scale bars = 5 μm.
Fig. 30. Longitudinal section through a cell.
Fig. 31. Cross-section through the lower cell half.

90, 100%), followed by chemical drying with hexamethyldisilazane (Carl Roth GmbH & Co KG, Karlsruhe, Germany) at room temperature for 20 min and finally at 50°C in a drying oven for 5 min. The filter was mounted on a stub and sputter coated with gold–palladium (SCD 050 Bal-Tec, Balzers, Liechtenstein). Cells were observed using a Tescan VEGA3 microscope (Elekronen-Optik-Service GmbH, Dortmund, Germany) at 15 kV using the SE detector.

For transmission electron microscopy (TEM), approximately 1 ml of *Plagiodinium belizeanum* culture was pelleted at 1000 revolutions per min and subsequently fixed in 2.5% glutaraldehyde in seawater on ice for 30 min, washed in seawater, and postfixed with 1% OsO_4 on ice for 1.5 h; both fixation steps were performed in the dark. After the fixation with OsO_4, samples were washed in seawater and dehydrated through a graded series of ethanol washes (30–100%) and acetone for 5 min at each step at room temperature. Samples were then placed in a 1:1 resin (Agar low-viscosity resin, Agar Sciences, Stansted, United Kingdom)/acetone mixture for 30 min, followed by a 100% resin mixture overnight at room temperature. Resin was exchanged the following day, and samples were polymerized at 68°C for 32 h. Samples were cut with a diamond knife and viewed with a Hitachi-7400 TEM.

For extracting genomic DNA and amplifying ribosomal (r)RNA genes, approximately 1 ml of the *Plagiodinium belizeanum* culture was pipetted into a 1.5-ml Eppendorf tube. Total genomic DNA was extracted following the manufacturer's protocol using a DNeasy blood and tissue kit (Qiagen, Germantown, Maryland USA). The primers SR1 5′-TACCTGGTTGATCCTGCCAG-3′ and SR5TAK 5′-ACTACGAGCTTTTTAACYGC-3′, as well as SR4 5′-AGGGCAAGTCTGGTGCCAG-3′ and SR12 5′-CCTTCCGCAGGTTCACCTAC-3′ (Nakayama *et al.* 1996) were used to amplify 18S rDNA sequences using the following program on a thermocycler: initial denaturation 94°C for 2 min; 35 cycles of 94°C for 30 s, 52°C for 30 s,

←
Figs 19, 20. Apical to right lateral view of the epitheca and cingulum.
Fig. 21. Apical view on the epitheca and cingulum with variable plate pattern (asterisk).
Fig. 22. Ventral to right lateral view on an epitheca with variable plate pattern (asterisk).
Figs 23, 24. Broken and isolated apical theca showing cingular plates (C1–C5) and some epithecal plates.
Fig. 25. Sulcal plates around the flagellar pore (fp).
Figs 26, 27. Sulcal and the two ventral hypothecal plates of a broken theca.
Figs 28, 29. Sulcal area of complete cells, showing the sulcal plates around the flagellar pore (fp).

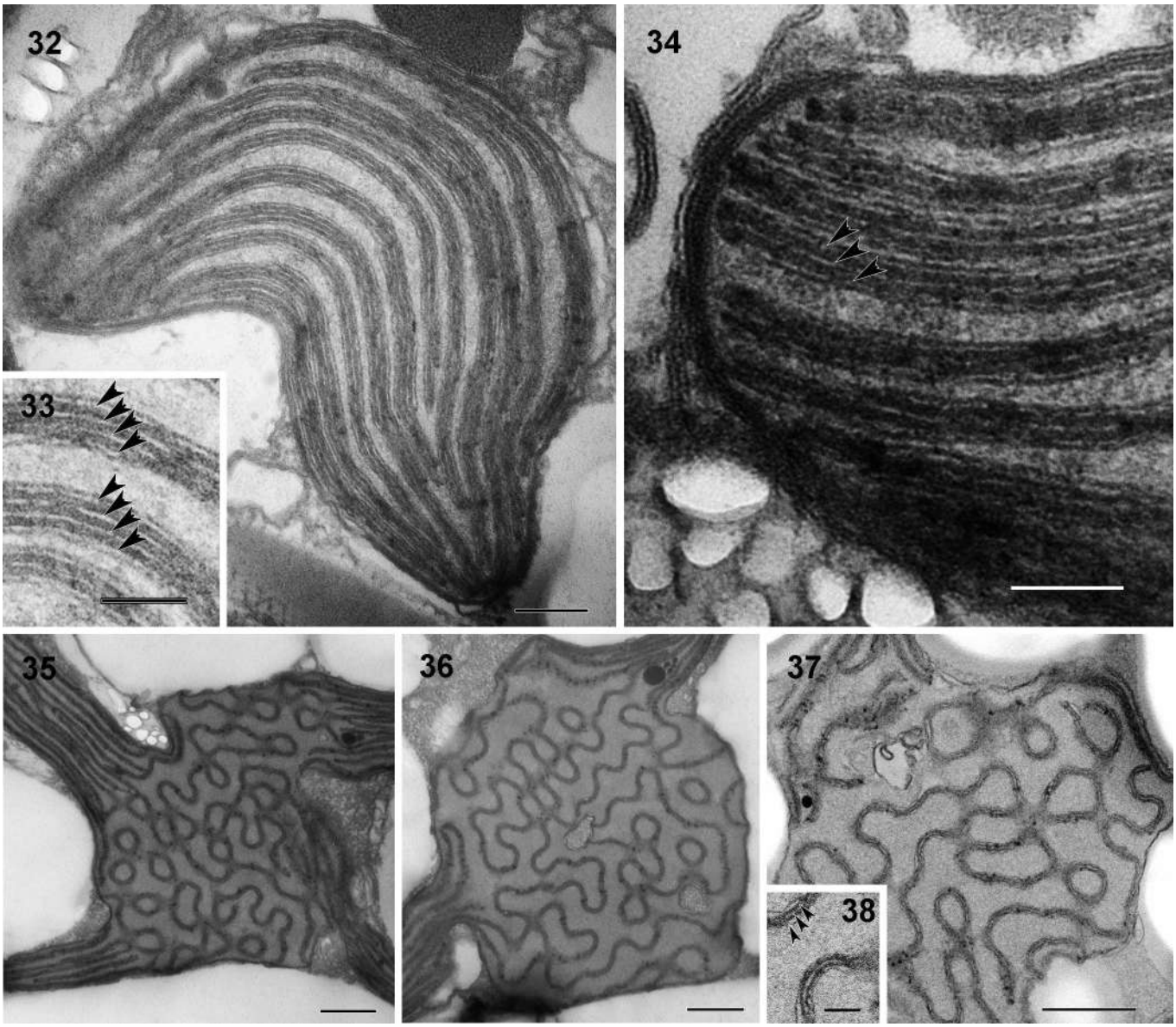

Figs 32–38. Transmission electron micrographs of *Plagiodinium belizeanum*.
Figs 32–34. Plastid and thylakoid details.
Fig. 32. Thylakoid lamellae in parallel order in the plastid. Scale bar = 200 nm.
Fig. 33. Detail of Fig. 32 showing thylakoids in stacks of four (arrowheads). Scale bar = 100 nm.
Fig. 34. Plastid detail with thylakoids in stacks of three (arrowheads). Scale bar = 100 nm.
Figs 35–37. Multistalked pyrenoids with thylakoids traversing the matrix. Scale bars = 500 nm.
Fig. 38. Detail for Fig. 37 showing the traversing thylakoids in stacks of three (arrowheads). Scale bar = 100 nm.

72°C for 1 min 30 s; final extension 72°C for 7 min. To amplify 28S rDNA sequences, the primers 25F1 5′-CCGCTGAATTTAAGCATAT-3′ and 25R1 5′-CTTGGTCCGTGTTTCAAGAC-3′, LSUD3A 5′-GACCCGTCTTGAAACACGGA-3′ and LSUR2 5′-ATTCGGCAGGTGAGTTGTTAC-3′ (Nunn *et al*. 1996; Kogame *et al*. 1999; Takano & Horiguchi 2005) were used in a reaction following the same thermocycler program described above. In each polymerase chain reaction (PCR), Econotaq 2× Mastermix (Lucigen, Middleton, Wisconsin USA) was used following the manufacturer's protocols. PCR products were purified using a Qiagen PCR purification kit; 1 µl of purified product was used in a sequencing reaction with ABI BigDye Terminator v1.1 (Applied Biosystems, Foster City, California USA) and subsequently purified with ethanol before being eluted in 18 µl of Hi-Di formamide (Applied Biosystems) and sequenced on a 3130 genetic analyzer (Applied Biosystems).

The newly obtained 18S and 28S rDNA sequences from *Plagiodinium belizeanum* were initially screened with the basic local alignment search tool (BLAST) tool, checking their affinity to other dinoflagellate lineages. These sequences were then aligned with 48 and 60 additional 18S and 28S sequences from other taxa, respectively, on the basis of the

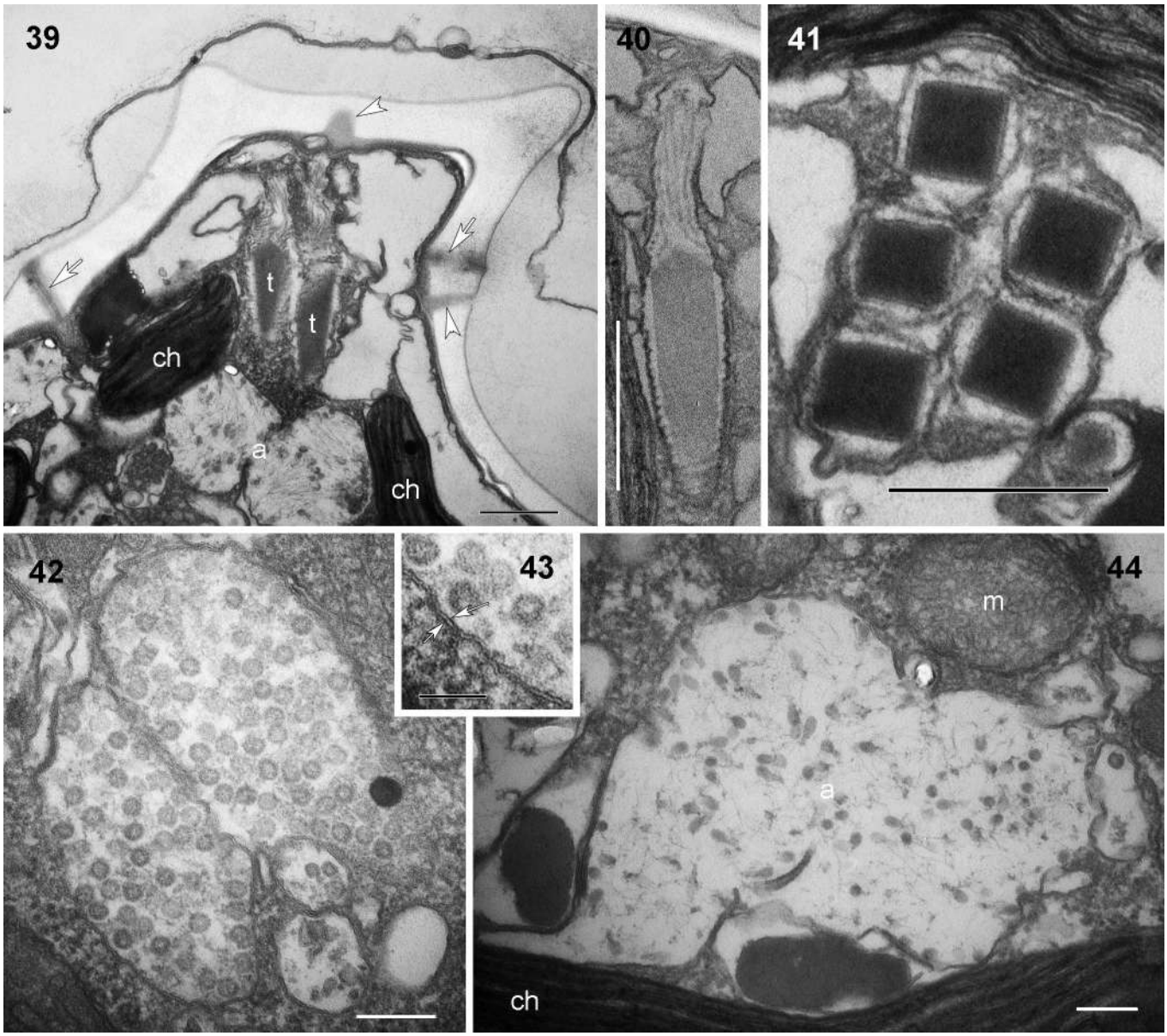

Figs 39–44. Transmission electron micrographs of *Plagiodinium belizeanum*.
Fig. 39. Longitudinal section through the epitheca with trichocysts (t) below the putative apical pore. Note the plate borders (arrows) and thecal pores (arrowhead). ch = plastid; a = autolysosome. Scale bar = 500 nm.
Fig. 40. Longitudinal section through a trichocyst. Scale bar = 500 nm.
Fig. 41. Cross-section through trichocysts. Scale bar = 500 nm.
Fig. 42. Autolysosome containing virus particles. Scale bar = 200 nm.
Fig. 43. Detail of Fig. 42 showing that the autolysosome is surrounded by two membranes (arrows). Scale bar = 100 nm.
Fig. 44. Autolysosome (a) with sparsely distributed, unidentified content. ch = plastid; m = mitochondrion. Scale bar = 200 nm.

initial BLAST/National Center for Biotechnology Information search. MUSCLE 3.8.31 was used to initially align both data sets (Edgar 2004). Alignments were subsequently edited and fine-tuned using Mesquite 3.04 (Maddison & Maddison 2015). Garli0.951-GUI (www.bio.utexas.edu/faculty/antisense/garli/Garli.html; Zwickl 2006) was used to run maximum-likelihood (ML) bootstrap analyses on both data sets. Jmodeltest 0.1.1 selected a general-time reversible (GTR + I + G) model of nucleotide substitutions under Akaike information criterion (AIC) and AIC with correction (AICc.) (Posada & Crandall 1998) that incorporated invariable sites and a discrete gamma distribution (eight categories) (GTR + Γ + I model: $\alpha = 0.5370$ and fraction of invariable sites = 0.300 for the 18S alignment, and $\alpha = 0.6480$ and fraction of invariable sites = 0.0670 for the 28S alignment). ML bootstrap analyses were performed on 500 pseudoreplicates, with one heuristic search per pseudoreplicate (Zwickl 2006), using the same program set to the GTR model + Γ + I. Bayesian analyses were performed using the program MrBayes 3.1.2 (Huelsenbeck & Ronquist 2001). The program was set to operate with GTR, a gamma-distribution and four Monte Carlo Markov chains (default

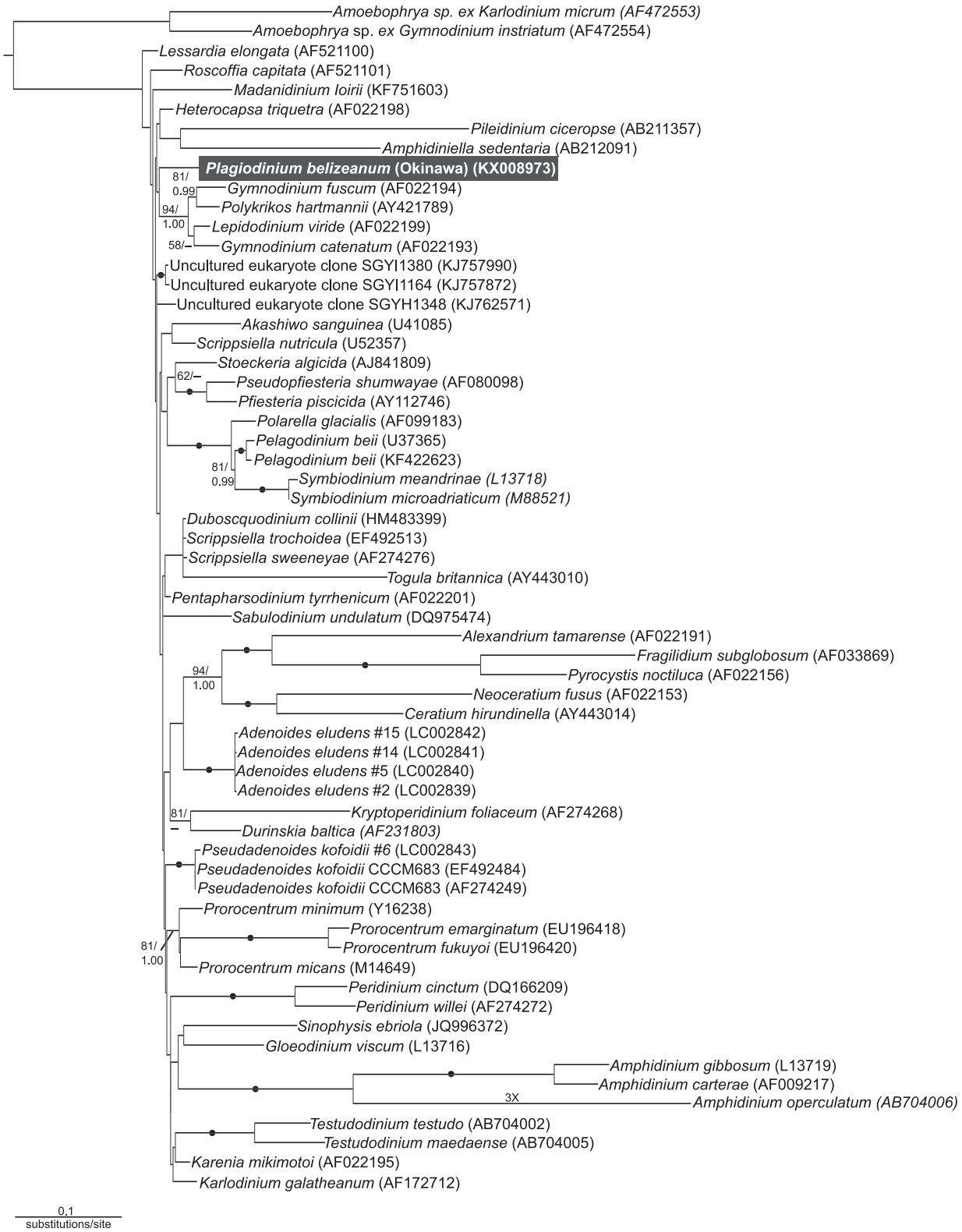

Fig. 45. Maximum likelihood (ML) and Bayesian inference derived from the phylogenetic analyses of 18S rDNA from *Plagiodinium belizeanum* and 60 other taxa representing the diversity of dinoflagellates over 1318 unambiguously aligned sites. This tree was inferred using the GTR + Γ + I substitution model (–ln L = 3726.2938, gamma shape = 0.4283, proportion of invariable sites = 0.3928). Numbers at the nodes denote the ML bootstrap percentage and Bayesian posterior probabilities, respectively. Black dots on branches denote instances where bootstrap support values and Bayesian posterior probabilities of 95/0.95 or higher were recorded. Bootstrap and Bayesian values less than 55 and 0.95 were not added to this tree. The novel sequence from *P. belizeanum* generated in this study is highlighted in a black box.

temperature = 0.2), with a total of 7,000,000 and 6,000,000 generations for the 18S and 28S alignments, respectively. Generations were calculated with trees sampled every 100 generations and with a prior burn-in of 1,000,000 generations (10,000 sampled trees were discarded; burn-in was checked manually). When the average split fell below 0.01, the program was set to terminate. All other parameters were left at the default setting. A majority rule consensus tree was constructed from 60,000 postburn-in trees for the 18S rDNA data set, whereas 50,000 trees were used for the 28S rDNA data set. Posterior probabilities correspond to the frequency at which a given node was found in the postburn-in trees.

RESULTS

Cells were laterally flattened, longer than deep, oval to oblong with a very small caplike episome, less deep than the hyposome, descending ventrally and tapering to the dorsal side (Figs 1, 4, 5). The plastid was yellow-brown (Fig. 1, 5). The chloroplast was located mainly at the cell periphery and many chloroplast lobes radiated from the cell centre as shown by autofluorescence (Figs 2, 6, 7). The round to oval nucleus was located in the posterior region of the cell (Figs 1, 3, 4). Starch granules of different sizes were distributed in the cell (Fig. 5). The transverse and longitudinal flagella were visible under the light microscope (Fig. 1), with the longitudinal flagellum about as long as the cell. Cells were 22–34 μm long ($n = 20$), 15–18 μm deep ($n = 20$), and 11–13 μm wide ($n = 20$). Smaller cells compared with the rest of cells in the culture were observed and they were 13–15 μm long ($n = 15$) and 6–8 μm deep ($n = 7$).

The thecal plates were smooth with scattered pores of two different size classes (Figs 8–27). Large pores were 95–100 nm in diameter and small pores 20–25 nm. The thecal plate pattern was Po 1′ 5′′ 5(6)C 4S 5′′′ 1′′′′ (Figs 8–29). The tiny epitheca consisted of seven plates (Figs 19, 20) with a ringlike apical pore plate in the centre (Fig. 19), a tiny first apical plate (1′) and five precingular plates (Figs 19, 20). The plate assignments were ambiguous and further interpretations were possible (see Discussion below). The ventral epithecal plate pattern was variable (Figs 21, 22, asterisks), with probable loss of plate 1′′ (Fig. 21) or fusion of plate 1′′ with the anterior sulcal plate (Fig. 22). The borders of the precingular plates ran down into the transverse furrow, so that they had a thick appearance in lateral view (Figs 19, 20, 22), especially the dorsal plate 3′′ (Figs 19, 23, 24). The deep cingulum completely encircled the cell without displacement (Figs 16, 17) and had five plates (Figs 19–23). The ventral cingular plates (C1 and C5) were relatively small, the lateral cingular plates (C2 and C4) were elongated/large and the dorsal cingular plate (C3) was of medium size (Figs 19, 21, 23). The division of C5 (Fig. 19) and C2 (Fig. 24) was observed, which resulted in six cingular plates. The sulcus consisted of four plates (Fig. 25) comprising only a short area where the cingulum ends meet (Figs 26–29), but the longitudinal furrow appeared longer (about half to two-thirds the hypotheca length) because of the ventral depression of the first postcingular plate (1′′′; Figs 16–18, 27). The sulcus was bordered by narrow marginal lists of plates 1′′′ and 5′′′ (Figs 16, 18, 29). The flagellar pore was surrounded by the anterior (Sa), the left, the posterior and the right sulcal plates (Figs 25, 26, 28, 29). The Sa plate was located as being part of the epitheca (Figs 19–21). The hypotheca consisted of five postcingular plates and one antapical plate (Figs 8–18). The two ventral postcingular plates (1′′′ and 5′′′) were relatively narrow and elongated (Figs 16–18). The two large lateral postcingular plates (2′′′ and 4′′′) covered nearly the complete lateral hypothecal sides (Figs 8–14). Plate 3′′′ was located dorsally (Fig. 15) and the antapical plate (1′′′′) covered the posterior cell end (Figs 8–16). Plate margins were simple lines (Figs 9, 11, 12) or intercalary bands that were wide with striation (Figs 10, 13, 14).

TEM revealed a plastid enveloped by three outer membranes (Fig. 34) and lobes radiating from a central pyrenoid (Figs 30, 31, 35). Thylakoids occurred in stacks of three or four (Figs 32–34). The multistalked pyrenoid was traversed by thylakoid stacks of three in an irregular manner, producing looplike structures (Figs 35–38). The cell also contained a conventional dinokaryon (Figs 30, 31), mitochondria (Fig. 44), accumulation bodies (Figs 30, 31) and starch grains (Figs 30, 31). Trichocysts were present and also positioned below the apical pore (Figs 39–41). Conspicuous double-membrane-bound sacks that were distinct from mitochondria were present throughout the cytoplasm (Figs 42–44). These putative autolysosomes sometimes contained numerous electron-dense spheres (Figs 42), but were occasionally observed containing comparatively little material (Figs 44). The electron-dense spheres stained positively with DAPI (Fig. 3 arrows).

In the phylogenetic tree inferred from 18S rDNA sequences, *Plagiodinium belizeanum* branched as a sister group to the *Gymnodinium sensu stricto* clade (containing *Gymnodinium fuscum*, *G. catenatum*, *Polykrikos hartmannii*, and *Lepidodinium viride*) without robust statistical support (Fig. 45). The phylogenetic tree inferred from 28S rDNA sequences showed a weakly supported branch between *Plagiodinium* and another benthic species, *Madanidinium loirii* (Fig. 46). Although the new 18S and 28S rDNA sequences are useful 'DNA bar codes' for *P. belizeanum*, molecular phylogenetic analyses of both data sets were unable to resolve the position of this species within dinoflagellates.

DISCUSSION

The cell shape, the episome and hyposome dimensions, the cell size range, the location of the nucleus and the presence of plastids agree with the original description of *Plagiodinium belizeanum* (Faust & Balech 1993). Sizes were given as 26.5–31.0 μm long, 20.0–24.5 μm wide, and 6.5–8.5 μm deep (Faust & Balech 1993). However, the width provided in the original description corresponds to the dorsoventral distance and should be the depth; similarly, the depth was initially measured between the lateral sides and should be the cell width. In light of these 'corrections', the sizes measured for the new isolate from Japan (13/22–34 μm long, 6/15–18 μm deep, 11–13 μm wide) were in the same range as the original

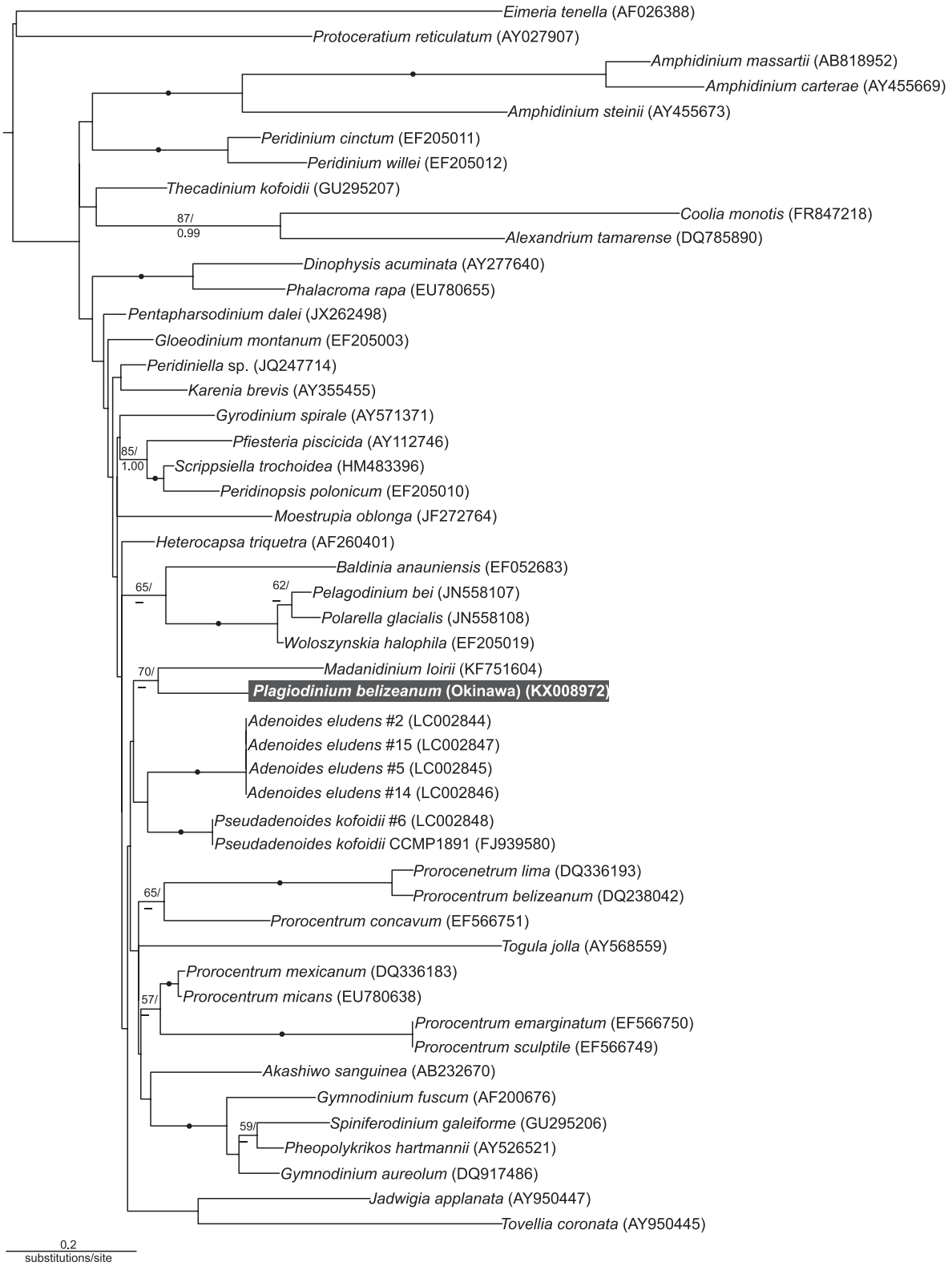

Fig. 46. Maximum likelihood (ML) and Bayesian inference derived from the phylogenetic analyses of 28S rDNA from *Plagiodinium belizeanum* and 48 other taxa representing the diversity of dinoflagellates over 675 unambiguously aligned sites. This tree was inferred using the GTR + Γ + I substitution model (–ln L = 1293.3928, gamma shape = 0.2356, proportion of invariable sites = 0.3942). Numbers at the nodes denote the ML bootstrap percentage and Bayesian posterior probabilities, respectively. Black dots on branches denote instances where bootstrap support values and Bayesian posterior probabilities of 95/0.95 or higher were recorded. Bootstrap and Bayesian values less than 55 and 0.95 were not added to this tree. The novel sequence from *P. belizeanum* generated in this study is highlighted in a black box.

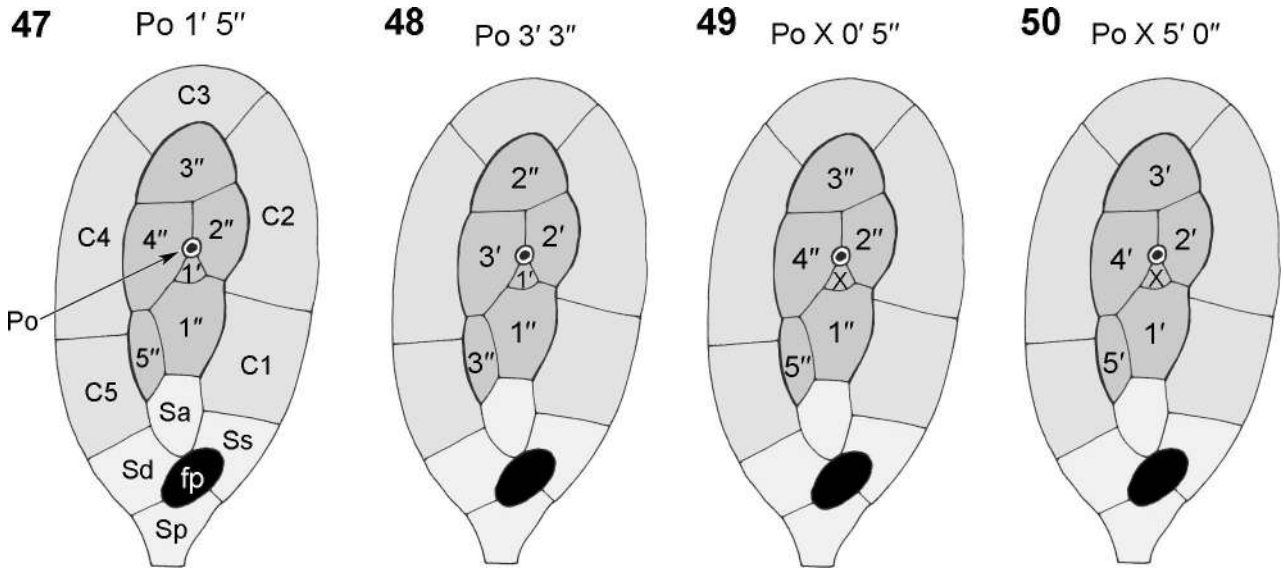

Figs 47–50. Drawings of possible plate tabulation interpretations in *Plagiodinium belizeanum*. Po = outer pore plate with apical pore; 1′–5′ = apical plate series; 1″–5″ = precingular plate series; X = canal plate; C1–C5 = cingular plate series; Sa = anterior sulcal plate; Ss = left sulcal plate; Sd = right sulcal plate; Sp = posterior sulcal plate; fp = flagellar pore.

description. Twenty-five fixed cells from a natural population were measured by Faust & Balech (1993). The larger range recorded herein might reflect culturing conditions and may contain multiple life-cycle stages, as a subset of distinctly smaller cells were observed in this culture.

Thecal reconstruction for the Japanese strain corresponds largely to the original description of *Plagiodinium belizeanum* (Faust & Balech 1993). However, an additional tiny apical plate (1′) was discovered ventral to the apical pore plate (Po). This resulted in the reinterpretation of the apical plate series (Faust & Balech 1993) as a precingular plate series (Fig. 47). This plate series assignment is supported by the plate borders running down into the transverse furrow (as in *Sabulodinium*, see below). Because the designation of the epithecal plates is ambiguous, several possible epithecal plate patterns can be considered (Figs 48–50). All plates in contact with the Po plate can be assigned as apical plates, leaving three disconnected plates (isolated dorsal plate; Fig. 48) in contact with the cingulum; therefore, these are considered precingular plates. The epitheca formula would be Po 3′ 3″ (Fig. 48). The tiny plate located ventral to the Po plate could also be interpreted as a canal plate (X), as in the Peridiniales, and then the complete series could be precingular plates (Fig. 49), resulting in a formula without apical plates: Po X 0′ 5″; or, that plate series comprised, as suggested by Faust & Balech (1993), apical plates (Po X 5′ 0″; Fig. 50). To demonstrate how ambiguous the epithecal plate interpretation is, a parallel to *Adenoides* can be discussed. *Adenoides* was reported to have five apical plates and six precingulars (Gómez *et al*. 2015), which seems very different from *Plagiodinium*. However, this could be a matter of interpretation, as the six precingulars in *Adenoides* can be compared with/named as cingular plates (possibly homologues) as in *Plagiodinium* or in *Pseudadenoides* (Hoppenrath *et al*. 2017). The remaining five apicals are similar in both genera, but not the apical pore complex. In the sulcal area, a flagellar pore was identified for the first time. It was located in the middle sulcal plate described by Faust & Balech (1993), which we could not reveal. The short and narrow sulcal lists described here were not recognized by Faust & Balech (1993). Thecal plates were smooth with scattered pores of two size classes. These discrepancies with the original description reflect delicate structures and matters of interpretation, so are not judged to be important traits for distinguishing different species.

Using LM, cells of *Plagiodinium* resemble species of *Amphidinium sensu stricto* but are clearly distinguished by their theca. Several laterally flattened thecate taxa with a small epitheca occur in benthic habitats (Hoppenrath *et al*. 2014). From these, three phototrophic species are most similar to *Plagiodinium*, namely *Thecadinium kofoidii* (Herdman) Larsen, *Pileidinium ciceropse* Tamura & Horiguchi and *Madanidinium loirii* Chomérat (Hoppenrath 2000; Tamura & Horiguchi 2005; Chomérat & Bilien 2014). *Thecadinium kofoidii* has only four postcingular plates and the antapical plate is located dorsally (Hoppenrath 2000). The epitheca tabulation is more complex (Po 3′ 1a 4″), including an elaborate apical pore plate and an anterior intercalary plate (Hoppenrath 2000). The precingular plate series is incomplete (not encircling the complete epitheca), starting on the dorsal side of the cell. This feature is distinctive and only shared with *Thecadiniopsis tasmanica* Croome, Hallegraeff & Tyler (Croome *et al*. 1987) and *Pseudothecadinium campbellii* Hoppenrath & Selina (Hoppenrath & Selina 2006). These two species have an asymmetrical and relatively larger epitheca with a descending cingulum (Croome *et al*. 1987; Hoppenrath & Selina 2006). Similarly to *Plagiodinium*, the anterior sulcal plate of *Thecadinium kofoidii* intrudes into the epitheca (Hoppenrath 2000). *Pileidinium ciceropse* has a similar hypothecal construction but is distinctly different through its incomplete cingulum (Tamura & Horiguchi 2005). The epitheca has also one apical plate and five precingular plates, like *Plagiodinium*, but plate 1′ is large, covering the epitheca center (Tamura & Horiguchi 2005). A

simple circular pore between plates 1′ and 2′′ was described (Tamura & Horiguchi 2005), resembling the Po of *Plagiodinium*. The sulcal area of *Pileidinium* is as small, as in *Plagiodinium*, with four plates encircling one flagellar pore.

Ultrastructurally, the pyrenoid morphology of *Pileidinium* resembles *Plagiodinium*, with thylakoids traversing the matrix in a manner also forming looplike structures (Tamura & Horiguchi 2005). *Madanidinium loirii* has a similar hypothecal construction but is distinctly different with its asymmetrical epitheca (Chomérat & Bilien 2014). The first postcingular plate has a depression extending the longitudinal furrow as in *Plagiodinium*. The sulcal area is moderately long and composed only of three plates – in contrast to *Plagiodinium* – but has also one oval flagellar pore (Chomérat & Bilien 2014). *Madanidinium* has no apical pore and the epitheca comprises 10 plates, with two apical, one anterior intercalary and seven precingular plates (Chomérat & Bilien 2014). This species was the sister lineage to *Plagiodinium* in the phylogenetic tree inferred from 28S rDNA sequences, albeit without convincing statistical support.

The heterotrophic *Sabulodinium* Saunders & Dodge is laterally flattened with a small epitheca with completely different thecal tabulation (Hoppenrath *et al*. 2007). The interesting similarity to *Plagiodinium* is the precingular plates with borders running down into the transverse furrow (Hoppenrath *et al*. 2007). To the best of our knowledge, this feature is known only from these two genera. *Planodinium striatum* Saunders & Dodge is a heterotrophic species with laterally flattened cells with small epitheca, with so far incompletely known thecal tabulation but with very different epithecal plate pattern and without apical pore (Hoppenrath *et al*. 2014). All these benthic genera have unusual epithecal plate patterns that are often difficult to interpret, some reduced with missing apical pores and missing or incomplete plate series. Sulcal constructions are often difficult to discern or to interpret, with unclear sulcal borders and plates running from the epitheca into the sulcus (Hoppenrath *et al*. 2014). The challenge of assigning tabulation patterns is exemplified by taxa such as *Pseudadenoides* F.Gómez, R.Onuma, Artigas & Horiguchi (Hoppenrath *et al*. 2003; Gómez *et al*. 2015; Hoppenrath *et al*. 2017) and some species of *Amphidiniopsis* Wołoszyńska (Hoppenrath *et al*. 2012, 2014).

The general ultrastructure of *Plagiodinium belizeanum* is typical for dinoflagellates: mitochondria with tubular cristae, a dinokaryon, trichocysts, and a plastid bounded by three membranes. Normally, the thylakoids are arranged in stacks of three in peridinin-containing plastids, but stacks of two or four were also recorded (e.g. Dodge 1975; Schnepf & Elbrächter 1999). Another study concluded through high-performance liquid chromatography analysis that *P. belizeanum* possesses a peridinin pigment (Yamada *et al*. 2015). It has been inferred that different types of pyrenoids are mainly species-level traits (e.g. Dodge & Crawford 1971; Schnepf & Elbrächter 1999; Hoppenrath & Leander 2008; Hoppenrath *et al*. 2017); however, some traits associated with pyrenoid ultrastructure reflect phylogenetic relationships above the species level (e.g. Hansen & Moestrup 1998; Hoppenrath *et al*. 2017). *Plagiodinium* has a so-called 'type D multi-stalked' pyrenoid (Dodge & Crawford 1971) that is most similar to the pyrenoids in *Pileidinium* (Tamura & Horiguchi 2005).

Double-membrane-bound autolysosomes filled with electron-dense spheres and polygons were common within the cytoplasm of *Plagiodinium*; we interpreted these electron-dense structures as virus particles. DAPI staining of fixed cells was consistent with this interpretation and showed that the putative virus-filled autolysosomes were distributed in patches throughout the cell. Viruses have been characterised from several other dinoflagellate genera, such as *Prorocentrum*, *Amphidinium*, *Alexandrium*, *Akashiwo*, *Cochlodinium, Gymnodinium* and *Heterocapsa* (Kim *et al*. 2012). Although some viral infections are located in sacks or distributed throughout the cytoplasm (Nagasaki *et al*. 2003), the putative viruses in our *Plagiodinium* culture were exclusively located within double-membrane-bound autolysosomes, a pattern reminiscent of the 'polyvesicle bodies' observed in *Pileidinium ciceropse* (Tamura & Horiguchi 2005). The role viruses play with their dinoflagellate hosts is not completely understood. Although thought to act primarily as pathogens, it has been proposed that viruses could confer some benefit (Lindell *et al*. 2007), namely by introducing genetic novelty to the host. Indeed, dinoflagellate nuclei contain viral nucleoproteins evidently derived from phycodnaviruses (Gornik *et al*. 2012; Janouškovec *et al*. 2016).

TAXONOMIC SUMMARY

Plagiodinium belizeanum Faust & Balech emend. Wakeman, Hoppenrath, Yamaguchi & Gavelis

Oval to oblong laterally flattened cells with very small caplike episome, less deep than the hyposome, descending ventrally and tapering to the dorsal side. Complete cingulum without displacement. Short sulcus with one flagellar pore. Cells are 13–34 μm long, 6–18 μm deep, 7–13 μm wide. Yellow-brown plastid, with three outer membranes and thylakoids in stacks of three or four, at the cell periphery radiating from the centre. Multistalked central pyrenoid traversed by thylakoid stacks. Posterior nucleus. Trichocysts present. Thecal plates smooth with scattered pores of two different size classes. Tabulation: Po 1′ 5′′ 5C 4S 5′′′ 1′′′′. Borders of precingular plates running down into the transverse furrow.

BAR CODES: Accession numbers (KX008973, KX008972).

GEOGRAPHY: Belize, Mexico, Malaysia, Japan.

ACKNOWLEDGEMENTS

We thank M. Schweikert, University of Stuttgart, Germany, for discussions on the ultrastructure, as well as the ALESS program at the University of Tokyo for financial assistance that partially aided in the collection of the samples. This work was also supported by grants to BSL from the National Science and Engineering Research Council of Canada (NSERC 2014-05258) and the Canadian Institute

for Advanced Research, Program in Integrated Microbial Biodiversity.

REFERENCES

Almazán-Becerril A., Escobar-Morales S., Rosiles-González G. & Valadez F. 2015. Benthic–epiphytic dinoflagellates from the northern portion of the Mesoamerican Reef System. *Botanica Marina* 58: 115–128.

Chomérat N. 2016. Studies on the benthic genus *Sinophysis* (Dinophysales, Dinophyceae): I. A taxonomic investigation from Martinique Island, including two new species and elucidation of the epithecal plate pattern. *Phycologia* 55: 445–461.

Chomérat N. & Bilien G. 2014. *Madanidinium loirii* gen. et sp. nov. (Dinophyceae), a new marine benthic dinoflagellate from Martinique Island, eastern Caribbean. *European Journal of Phycology* 49: 165–178.

Chomérat N., Couté A. & Nézan E. 2010. Further investigations on the sand-dwelling genus *Cabra* (Dinophyceae, Peridiniales) in South Brittany (northwestern France), including the description of *C. aremorica* sp. nov. *Marine Biodiversity* 40: 131–142.

Croome R.L., Hallegraeff G.M. & Tyler P.A. 1987. *Thecadiniopsis tasmanica* gen. et sp. nov. (Dinophyta: Thecadiniaceae) from Tasmanian freshwater. *British Phycological Journal* 22: 325–333.

Dodge J.D. 1975. A survey of chloroplast ultrastructure in the Dinophyceae. *Phycologia* 14: 253–263.

Dodge J.D. & Crawford R.M. 1971. A fine-structural survey of dinoflagellate pyrenoids and food-reserves. *Botanical Journal of the Linnean Society* 64: 105–115.

Edgar R.C. (2004) MUSCLE: multiple sequence alignment with high accuracy and high throughput. *Nucleic Acids Research* 35: 1792–1797.

Faust M.A. & Balech E. 1993. A further SEM study of marine benthic dinoflagellates from a mangrove island, Twin Cays, Belize, including *Plagiodinium belizeanum* gen. et sp. nov. *Journal of Phycology* 29: 826–832.

Gómez F., Onuma R., Artigas L.F. & Horiguchi T. 2015. A new definition of *Adenoides eludens*, an unusual marine sand-dwelling dinoflagellate without cingulum, and *Pseudadenoides kofoidii* gen. & comb. nov. for the species formerly known as *Adenoides eludens*. *European Journal of Phycology* 50: 125–138.

Gornik S.G., Ford K.L., Mulhern T.D., Bacic A., McFadden G.I. & Waller R. 2012. Loss of nucleosomal DNA condensation coincides with appearance of a novel nuclear protein in dinoflagellates. *Current Biology* 22: 2303–2312.

Hansen G. & Moestrup Ø. 1998. Light and electron microscopical observations on *Peridiniella catenata* (Dinophyceae). *European Journal of Phycology* 33: 293–305.

Hoppenrath M. 2000. Morphology and taxonomy of the marine sand-dwelling genus *Thecadinium* (Dinophyceae), with the description of two new species from the North German Wadden Sea. *Phycologia* 39: 96–108.

Hoppenrath M. 2017. Dinoflagellate taxonomy – a review and proposal of a revised classification. *Marine Biodiversity* 47: 381–403.

Hoppenrath M. & Leander B.S. 2008. Morphology and molecular phylogeny of a new marine sand-dwelling *Prorocentrum* species, *P. tsawwassenense* (Dinophyceae, Prorocentrales), from British Columbia, Canada. *Journal of Phycology* 44: 451–466.

Hoppenrath M. & Selina M. 2006. *Pseudothecadinium campbellii* gen. nov. et sp. nov. (Dinophyceae), a phototrophic, thecate, marine planktonic species found in the Sea of Okhotsk, Russia. *Phycologia* 45: 260–269.

Hoppenrath M., Schweikert M. & Elbrächter M. 2003. Morphological reinvestigation and characterization of the marine, sand-dwelling dinoflagellate *Adenoides eludens* (Dinophyceae). *European Journal of Phycology* 38: 385–394.

Hoppenrath M., Horiguchi T., Miyoshi Y., Selina M., Taylor F.J.R. & Leander B.S. 2007. Taxonomy, phylogeny, biogeography, ecology of *Sabulodinium undulatum*, including an amended description of the species. *Phycological Research* 55: 159–175.

Hoppenrath M., Selina M., Yamaguchi A. & Leander B.S. 2012. Morphology and molecular phylogeny of *Amphidiniopsis rotundata sp. nov.* (Peridiniales, Dinophyceae), a benthic marine dinoflagellate. *Phycologia* 51: 157–167.

Hoppenrath M., Murray S.A., Chomérat N. & Horiguchi T. 2014. *Marine benthic dinoflagellates – unveiling their worldwide biodiversity*. Kleine Senckenberg-Reihe 54, E. Schweizerbart'sche Verlagsbuchhandlung (Nägele u. Obermiller), Stuttgart. 276 pp.

Hoppenrath M., Yubuki N., Stern R. & Leander B.S. 2017. Ultrastructure and molecular phylogenetic position of a new marine sand-dwelling dinoflagellate from British Columbia, Canada: *Pseudadenoides polypyrenoides* sp. nov. (Dinophyceae). *European Journal of Phycology* 52: 208–224.

Horiguchi T. 1995. *Amphidiniella sedentaria* gen. et sp. nov. (Dinophyceae), a new sand-dwelling dinoflagellate from Japan. *Phycological Research* 43: 93–99.

Huelsenbeck J.P. & Ronquist F. 2001. MRBAYES:Bayesian inference of phylogenetic trees. *Bioinformatics* 17: 754–755.

Janouškovec J., Gavelis G.S., Burki F., Dinh D., Bachvaroff T.R., Gornik S.G., Bright K.J., Imanian B., Strom S.L., Delwiche C.F., Waller R.F., Fensome R.A., Leander B.S., Rohwer F.L. & Saldarriaga J.F. 2016. Major transitions in dinoflagellate evolution unveiled by phylotranscriptomics. *Proceedings of the National Acadamy of Sciences of the United States of America* 114(2): E171–E180.

Kim J., Kim C.-H., Takano Y., Jang I.-K., Kim S.W. & Choi T.-J. 2012. Isolation and physiological characterisation of a new algicidal virus infecting the harmful dinoflagellate *Heterocapsa pygmaea*. *Plant Pathology Journal* 28: 433–438.

Kogame K., Horiguchi T. & Masuda M. 1999. Phylogeny of the order Scytosiphonales (Phaeophyceae) based on DNA sequence of rbcL, partial rbcS, and partial LSU nrDNA. *Phycologia* 38: 496–502.

Lindell D., Jaffe J.D., Coleman M.L., Futschik M.E., Axmann I.M., Rector T., Kettler G., Sullivan M.B., Sten R., Hess W.R., Church G.M. & Chisholm S.W. 2007. Genome-wide expression dynamics of a marine virus and host reveal features of co-evolution. *Nature* 449: 83–86.

Maddison W.P. & Maddison D.R. 2015. Mesquite: a modular system for evolutionary analysis. Version 3.04 http://mesquiteproject.org.

Murray S. & Patterson D.J. 2004. *Cabra matta*, gen. nov., sp. nov., a new benthic, heterotrophic dinoflagellate. *European Journal of Phycology* 39: 229–234.

Murray S., Hoppenrath M., Preisfeld A., Larsen J., Yoshimatsu S., Toriumi S. & Patterson D.J. 2006. Phylogenetics of *Rhinodinium broomeense* gen. et sp. nov., a peridinoid, sand-dwelling dinoflagellate (Dinophyceae). *Journal of Phycology* 42: 934–942.

Nagasaki K., Tamaru Y., Tarutani K., Katanozaka N., Yamanaka S., Tanabe H. & Yamaguchi M. 2003. Growth characteristics and intraspecies host specificity of a large virus infecting the dinoflagellate *Heterocapsa circularisquama*. *Applied Environmental Microbiology* 69: 2580–2580.

Nakayama T., Watanabe S., Mitsui K., Uchida H. & Inouye I. 1996. The phylogenetic relationship between the Chlamydomonadales and Chlorococcales inferred from 18S rDNA sequence data. *Phycological Research* 44: 47–55.

Nunn G.B., Theisen B.F., Christensen B. & Arctander P. 1996. Simplicity-correlated size growth of the nuclear 28S ribosomal RNA D3 expansion segment in the crustacean order Isopoda. *Journal of Molecular Evolution* 42: 211–223.

Okolodkov Y.B., Merino-Virgilio F.D.C., Aké-Castillo J.A., Aguilar-Trujillo A.C., Espinosa-Matías S. & Herrera-Silveira A. 2014. Seasonal changes in epiphytic dinoflagellate assemblages near the northern coast of the Yucatan Peninsula, Gulf of Mexico. *Acta Botanica Mexicana* 107: 121–151.

Posada D. & Crandall K.A. 1998. JMODELTEST: testing the model of DNA substitution. *Bioinformatics* 14: 817–818.

Saburova M. & Chomérat N. 2014. *Ailadinium reticulatum* gen. et sp. nov. (Dinophyceae), a new thecate, marine, sand-dwelling dinoflagellate from the northern Red Sea. *Journal of Phycology* 50: 1120–1136.

Saunders R.D. & Dodge J.D. 1984. An SEM study and taxonomic revision of some armoured sand-dwelling marine dinoflagellates. *Protistology* 20: 271–283.

Schnepf E. & Elbrächter M. 1999. Dinophyte chloroplasts and phylogeny – a review. *Grana* 38: 81–97.

Takano Y. & Horiguchi T. 2005. Acquiring scanning electron microscopical, light microscopical and multiple gene sequence data from a single dinoflagellate cell. *Journal of Phycology* 42: 251–256.

Tamura M. & Horiguchi T. 2005. *Pileidinium ciceropse* gen. et sp. nov. (Dinophyceae), a sand-dwelling dinoflagellate from Palau. *European Journal of Phycology* 40: 281–291.

Taylor F.J.R., Hoppenrath M. & Saldarriaga J.F. 2008. Dinoflagellate diversity and distribution. *Biodiversity and Conservation* 17: 407–418.

Yamada N., Tanaka A. & Horiguchi T. 2015. Pigment compositions are linked to the habitat types in dinoflagellates. *Journal of Plant Research* 128: 923–932.

Zwickl D. 2006. *Genetic algorithm approaches for the phylogenetic analysis of large biological sequence data sets under the maximum likelihood criteria*. PhD thesis. University of Texas at Austin.

Received 7 April 2017; accepted 22 August 2017